


RESEARCH

Open Access



Lactate accumulation promotes immunosuppression and fibrotic transformation of bone marrow microenvironment in myelofibrosis

Mariarita Spampinato^{1†}, Cesarina Giallongo^{2†}, Sebastiano Giallongo², Enrico La Spina¹, Andrea Duminuco³, Lucia Longhitano¹, Rosario Caltabiano⁴, Lucia Salvatorelli⁴, Giuseppe Broggi⁴, Elisabetta P. Pricoco⁵, Vittorio Del Fabro³, Ilaria Dulcamare⁶, Antonio Massimo Di Mauro⁷, Alessandra Romano⁸, Francesco Di Raimondo⁸, Giovanni Li Volti^{1*} , Giuseppe A. Palumbo^{2†} and Daniele Tibullo^{1†}

Abstract

Background Clonal myeloproliferation and fibrotic transformation of the bone marrow (BM) are the pathogenetic events most commonly occurring in myelofibrosis (MF). There is great evidence indicating that tumor microenvironment is characterized by high lactate levels, acting not only as an energetic source, but also as a signaling molecule.

Methods To test the involvement of lactate in MF milieu transformation, we measured its levels in MF patients' sera, eventually finding a massive accumulation of this metabolite, which we showed to promote the expansion of immunosuppressive subsets. Therefore, to assess the significance of its trafficking, we inhibited monocarboxylate transporter 1 (MCT1) by its selective antagonist, AZD3965, eventually finding a mitigation of lactate-mediated immunosuppressive subsets expansion. To further dig into the impact of lactate in tumor microenvironment, we evaluated the effect of this metabolite on mesenchymal stromal cells (MSCs) reprogramming.

Results Our results show an activation of a cancer-associated phenotype (CAF) related to mineralized matrix formation and early fibrosis development. Strikingly, MF serum, enriched in lactate, causes a strong deposition of collagen in healthy stromal cells, which was restrained by AZD3965. To corroborate these outcomes, we therefore generated for the first time a TPO^{high} zebrafish model for the establishment of experimental fibrosis. By adopting this model, we were able to unveil a remarkable increase in lactate concentration and monocarboxylate transporter 1 (MCT1) expression in the site of hematopoiesis, associated with a strong downregulation of lactate export channel

[†]Mariarita Spampinato, Cesarina Giallongo, Giuseppe A. Palumbo and Daniele Tibullo contributed equally to this work.

*Correspondence:
Giovanni Li Volti
livolti@unict.it

Full list of author information is available at the end of the article



© The Author(s) 2025. **Open Access** This article is licensed under a Creative Commons Attribution-NonCommercial-NoDerivatives 4.0 International License, which permits any non-commercial use, sharing, distribution and reproduction in any medium or format, as long as you give appropriate credit to the original author(s) and the source, provide a link to the Creative Commons licence, and indicate if you modified the licensed material. You do not have permission under this licence to share adapted material derived from this article or parts of it. The images or other third party material in this article are included in the article's Creative Commons licence, unless indicated otherwise in a credit line to the material. If material is not included in the article's Creative Commons licence and your intended use is not permitted by statutory regulation or exceeds the permitted use, you will need to obtain permission directly from the copyright holder. To view a copy of this licence, visit <http://creativecommons.org/licenses/by-nc-nd/4.0/>.

MCT4. Notably, exploiting MCTs expression in biopsy specimens from patients with myeloproliferative neoplasms, we found a loss of MCT4 expression in PMF, corroborating changes in MCT expression during BM fibrosis establishment.

Conclusions In conclusion, our results unveil lactate as a key regulator of immune escape and BM fibrotic transformation in MF patients, suggesting MCT1 blocking as a novel antifibrotic strategy.

Keywords Lactate, Myelofibrosis, Tumor microenvironment, Monocarboxylate transporters

Introduction

Myelofibrosis (MF) is a severe subtype of myeloproliferative neoplasm (MPN) characterized by clonal proliferation of hematopoietic stem cells, bone marrow (BM) fibrosis, extramedullary hematopoiesis, splenomegaly, aberrant inflammation and an inherent risk of blastic transformation [1]. Currently, the treatment with JAK inhibitors (JAKi) has benefits in terms of spleen size control, and symptoms mitigation, eventually improving the quality of life, and prolonging patients' overall survival [2–4], especially in those classified as high risk according to standard prognostic scores [5]. However, the disease-modifying potential of JAKi therapy is limited, and the only potentially curative treatment is allogeneic hematopoietic stem cell transplantation [6], even if new helpful approaches are under evaluation above all in anemic [7] and JAKi refractory patients [8]. The disease arises *de novo* as primary MF (PMF), or it might occur post polycythemia vera (PV) or post essential thrombocythemia (ET). In this context, 90% of patients carry JAK2, CALR or MPL mutations, which are indeed defined as “driver” mutations [9]. Interestingly, MF pathophysiology is deeply influenced by alterations in the BM microenvironment, highlighted by BM fibrosis, neo-angiogenesis and osteosclerosis [10, 11]. The hallmark feature of MF is indeed the excessive extracellular matrix (ECM) deposition, causing a progressive loss of hematopoiesis and splenomegaly due to extramedullary hematopoiesis. In particular, BM fibrosis occurs as a cytokine-mediated secondary reaction toward the starting clonal malignant expansion, leading to overbalanced ECM deposition [12, 13].

In this context, mesenchymal stromal cells (MSCs) interact with megakaryocytes (MK), in turn releasing profibrotic cytokines as tumor growth factor beta (TGF- β). As a result, MKs prompt MSCs to differentiate into fibroblasts, acquiring a fibronectin-secreting phenotype [13, 14]. In particular, multipotent mesenchymal progenitor cells are the predominant type I collagen-producing cells in overt BM fibrosis [15]. Over time, all MSC subsets are functionally reprogrammed losing their hematopoietic supportive capacity and secreting non-collagenous ECM as a scaffold for collagen fibrosis [15]. Moreover, MSCs are pushed toward osteogenic differentiation supporting MF pathophysiology [12, 16].

Genetic and epigenetic changes are often coupled with metabolic reprogramming of cancer cells in order to fuel their increased energy demands [17, 18]. This leads to a nutrient competition between cancer cells and the surrounding stromal cells as well as the immune compartment, potentially promoting immune escape mechanisms and reprogramming of the whole BM niche in favor of tumor cell proliferation [19, 20]. Enhanced glycolysis, even under aerobic conditions, which is known as Warburg effect, is one of the hallmarks of cancer cells [18, 21]. This metabolic alteration is more closely related to the deregulations of molecular pathways controlling glucose uptake than mitochondria defects [22]. Lactate dehydrogenase A (LDHA), which catalyzes pyruvate-to-lactate conversion, has a central role in glycolysis, and, in several models, it has been related to tumor progression [23, 24]. Consistent with these observations, LDH levels are typically increased in MF patients' sera and predicts shorter overall and leukemia-free survival [25]. Moreover, JAK2-V617F mutant cells increase glucose uptake and glycolysis through STAT5 activation, required for JAK2-V617F mediated transformation [19, 26, 27]. Interestingly, selective inhibition of 6-phosphofructo-2-Kinase activity induced apoptosis in primary cells from patients and antagonized the disease phenotype of JAK2-mutant MPN mice [28]. The deregulation of intracellular and extracellular metabolites associated to cancer metabolic reprogramming also affects cellular transcriptome, secretome, and differentiation, eventually reshaping the whole tumor microenvironment (TME) [29]. In this context, the excess of lactate secreted by cancer cells as a consequence of the Warburg's effect itself, promotes angiogenesis, immune suppression and cancer-associated fibroblast (CAF) activation [20, 30–33]. Similarly, an association between plasmatic LDH and the severity of idiopathic pulmonary fibrosis has been described [34, 35]. Recently, it has been suggested that lactate from pancreatic cancer cells increases the number of CAF, which promote fibrotic tumor formation [36]. The role of lactate in TME reshaping also involves its role as epigenetic regulator. In hepatocellular carcinoma, lysine lactylation at specific sites, such as K28, plays a crucial role in promoting tumor proliferation and metastasis [37]. Additionally, lactylation influences critical cellular processes like glycolysis and macrophage polarization, further supporting tumor progression and immune modulation [38].

Although the characterization of tumor metabolism has been described, insights on how changed TME metabolic composition is in MF patients, is poorly understood. Here, we showed that the amount of circulating lactate increases in MF patients, eventually promoting the expansion of immunosuppressive subsets and fibrosis development. Accordingly, these effects are restrained by blocking lactate import channel monocarboxylate transporter 1 (MCT1). We also demonstrated that the expression of lactate export channel monocarboxylate transporter 4 (MCT4) in TME is deeply remodeled during fibrotic transformation, suggesting a link between lactate trafficking and pro-fibrotic establishment.

Materials and methods

Sample collection, cell cultures and treatments

Peripheral blood (PB) samples were collected from MF patients and age-matched controls after written informed consent (Azienda Ospedaliero-Universitaria Policlinico “G.Rodolico-San Marco”, n. 54/2022/PO). Clinical data of patients included in this study are shown in Table 1. Peripheral blood mononuclear cells (PBMCs) were obtained from healthy donor buffy coats after separation by Ficoll-Hypaque gradient.

Commercially available stromal cell lines HS-5 were grown in DMEM supplemented with 10% FBS and 1% penicillin-streptomycin. Osteoblastic differentiation was induced culturing HS-5 cells with a osteogenic induction medium (OIM): DMEM 10% FBS, 1%

Table 1 Clinical characteristic of PMF patients (n = 22) included in the study

Median years of age (range)	67 (40–76)
Sex	16 M (69%), 7 F (31%)
Blood count	
-Hb, g/dL (range)	10.2 (6.1–17.2)
-WBC, x10 ³ /mmc (range)	9.7 (1.2–149.1)
-Platelets, x10 ³ /mmc (range)	349 (70–1016)
Blast > 5%	2 (9.1%)
BM fibrosis	
-0	3 (13.04%)
-1	11 (47.82%)
-2	6 (26.09%)
-3	3 (13.04%)
Driver mutations	
-JAK2	15 (65.2%)
-CALR	3 (13.05%)
-MPL	0
-Triple negative	3 (13.05%)
-Not available	2 (8.7%)
IPSS/MYSEC-PM	
-Low	2 (8.7%)
-Intermediate-1	6 (26.08%)
-Intermediate-2	10 (43.48%)
-High	5 (21.74%)

Hb: hemoglobin; WBC=white blood cells; IPSS/MYSEC-PM=International Prognostic Scoring System/MYSEC Prognostic Model Risk Calculator

penicillin-streptomycin, 10 mM b-glycerophosphate (Calbiochem, San Diego, CA, USA), 0.2 mM ascorbic acid and 0.1 mM dexamethasone (Sigma-Adrich, Mylan, Italy). The medium was replaced every 3 days.

Sodium lactate (20 mM) and AZD3965 (10 μ M) were obtained from Sigma-Adrich (Mylan, Italy) and Selleckchem (Cologne, Germany) respectively.

Lactate concentration measurement

Spectrophotometric determination of lactate was carried out as previously described [39]. Briefly, the reaction mixture contained 100 mM Tris-HCl, 1.5 mM N-ethyl-N-2-hydroxy-3-sulfopropyl-3-methylalanine, 1.7 mM 4-aminoantipyrine and 5 International Unit (IU) horseradish peroxidase. Fifty microliters of serum were added to the mixture. The reaction was started with the addition of 5 IU of lactate oxidase to the cuvette (finale volume = 1 ml) and it was considered ended when no change in absorbance was recorded for at least 3 min. To calculate lactate in serum samples, the difference in absorbance at 545 nm wavelength (Δ abs) of each sample was interpolated with a calibration curve obtained by plotting Δ abs measured in standard solutions of lactate with increasing known concentrations.

Flow cytometry

For regulatory T cells (Treg) analysis, immune cells were stained with CD4-PEVio770 (clone SFC112T4D11), CD25-APC (clone B1.49.9) and FOXP3-PE (clone 259D), all from Beckman Coulter, and Treg were defined as CD4⁺CD25^{high}FOXP3⁺. For monocytic myeloid derived suppressor cells (M-MDSCs) analysis, immune cells were stained with CD14-FITC (clone 322 A.1, TLY4) and HLA-DR-APC (clone Immu-357) [40], all from Beckman Coulter, and M-MDSCs were defined as CD14⁺HLA-DR⁺.

qPCR

After RNA extraction, reverse transcription was performed by using the high-capacity cDNA Reverse Transcription Kit (Thermo Fisher Scientific, Milan, Italy). Then the relative transcription of human genes MCT1 (Fw: TGTTGTTGCAAATGGAGTGT; Rw: AAGTCGA TAAT- GATGCCCATGCCAA), MCT4 (Fw: TATCCA GATCTACCTCACCAC; Rw: GGCCTGGCAAAGATG TCGATGA) was determined by RTqPCR using Brilliant III Ultra-Fast SYBR Green QPCR Master Mix (Agilent Technologies, Milan, Italy) and 7900HT Fast Real-Time PCR System (Thermo Fisher Scientific). For each sample, the relative expression level of the mRNA of interest was determined by comparison with the control housekeeping gene B2M (Fw: AGCAGCATCATGGAGGTTTG; Rw: AGCCCTCCTAGAGC- TACCTG) using the $2^{-\Delta\Delta C_t}$ method.

Western blot

As previously described [41], extracted proteins were loaded onto a 12% polyacrylamide gel Mini-PROTEAN TGXTM (BIO-RAD, Milan, Italy) followed by electro-transfer to nitrocellulose membrane Trans-Blot TurboTM (BIO-RAD) using Trans-Blot SE Semi-Dry Transfer Cell (BIO-RAD) [42]. After blocking membranes were incubated with primary antibodies against human Col1A (sc-59772, Santa Cruz Biotechnology, Texas, USA), α SMA, PDGFR β , FAP, β -actin (ab15734, ab32570, ab207178 and ab181602 respectively; Abcam, Mylan, Italy). Next day, infrared anti-mouse IRDye800CW and antirabbit IRDye700CW secondary antibodies (Licor Biotechnology, Cambridge, United Kingdom) were used. Proteins bands were visualized using Odyssey Infrared Imaging Scanner (Licor Biotechnology). The density of each band was quantified using ImageJ analysis software and normalized to protein levels of β -actin.

Cytokine and chemokine detection

Multiplex immunobead assay technology (procartaplex Cytokine/Chemokine Magnetic Bead Panel, of Thermo Scientific, MA, Usa and Magpix analytical test instrument of Luminex Corp., Austin, TX) was performed on culture medium to determine concentrations of selected cytokines (Bone morphogenetic protein 2 (BMP2), osteopontin, calcitonin, Receptor activator of nuclear factor kappa-B ligand (sRANKL), matrix metalloproteinase 2 (MMP2), matrix metalloproteinase 9 (MMP9) chitinase 3 like 1 (CHI3L1), Regulated upon activation, normal T cell expressed and secreted (RANTES/CCL5).

Cell mineralization

HS-5 cells were incubated with 2% Alizarin Red S (Sigma-Aldrich) for 10 min. After washing, cell mineralization was evaluated by using a phase-contrast microscopy.

Mallory's trichrome staining

Cells were stained in 1% fuchsin acid (Sigma-Adrich) solution in distilled water; then, they were counterstained with a solution of 0.5% aniline blue (Sigma-Adrich), 2% orange G (Sigma-Adrich) and 2% oxalic acid (Sigma-Adrich) in distilled water. The standard methods were applied as previously described by Wołun-Cholewa et al. [43].

Immunofluorescence

Cells were fixed using 4% paraformaldehyde (PFA) prior to permeabilization. Primary antibody against human Col1A1 (sc-59772) and MCT4 (Abcam; ab234728) were used. After 24 h, cells were washed and incubated with an anti-mouse secondary antibody Alexa Fluor 647 for 1 h at room temperature. After washing, nuclei were counterstained with DAPI for 5 min, at room temperature.

Slices were mounted with fluorescent mounting medium Permafluor (Thermo Fisher Scientific) and digital images were acquired using a Zeiss Axio Imager Z1 Microscope with Apotome 2 system (Zeiss, Milan, Italy).

Immunohistochemistry

The immunohistochemical analyses were performed as previously described [44]. After proper deparaffinization and pretreatments, the slides were incubated with primary antibodies against CD90 (Abcam; ab181469), MCT1 (Abcam; ab90582) and MCT4 (Abcam; ab234728). Sections were counterstained with hematoxylin and evaluated with a light microscope (Carl Zeiss, Oberkochen, Germany). Both MCT1 and MCT4 were assessed as positive if chromogen was found in the cellular cytoplasm with or without nuclear staining. CD90 was considered as positive if chromogen was found in the cellular membranes and/or cytoplasm.

In vivo zebrafish model

Ethics statement

The experimental procedures were approved by the Animal Studies Committee of Ministero della Salute Italy (Approval code: 30/2022-PR). All of the procedures were performed according to the relevant regulations.

Zebrafish husbandry

Adult wildtype (5–8-months-old) AB zebrafish were used for this study. Fishes were housed at a density of five fishes per tank in mixed-sex groups in 2.5 L tanks on a recirculating system in 28 °C water in a room with a 14:10 h light: dark cycle. System water was carbon-filtered municipal tap water, filtered through a 20 μ m pleated particulate filter, and exposed to 40 W UV light [45]. Standard feeding protocol was three meals daily of Tetra-Min (Tetra) in the CAPIR (University of Catania) facility.

TPO^{high} zebrafish model, cell collection and flow cytometry

TPO^{high} zebrafish cohort was exposed to 100 μ g/kg Eltrombopag Olamine (Selleckchem, Cologne, Germany) every 3 day. Control and TPO^{high} zebrafish were anaesthetized after 15 days with 0.02% tricaine before kidney marrow collection. After a ventral, midline incision was made, kidney marrow was dissected and placed into ice-cold PBS containing 5% FBS. Whole kidney marrow (WKM) cells were passed through a filter with a 40- μ m pore size. Propidium iodide (Sigma) was added to exclude dead cells and debris. Flow cytometry analysis and sorting was based on propidium iodide exclusion, forward scatter and side scatter as previously described [39]. WKM cells were also transferred onto a slide by cytocentrifugation and stained with May-Grunwald-Giemsa.

RT-qPCR

Total RNA was extracted from WKM by Trizol reagent. After reverse transcription, we evaluated expression of the following zebrafish mRNA: *cd41* (FW: CTGAAGG CACTAACGTCAAC; RW: TCCTTCTTCTGACCAGAGTTA), *mpl* (FW: CGCCAACCAAGCCAGAGTTA; RW: ACTTTTCAACAGGTGCATCCCA), *tgfb1* (FW: TTCGTCTTCCAGCAAGCTCA; RW: TGGAGACAA AGCGAGTTCCC), *col1a1* (FW: ACCCTTAAGTCCCT GAGCCA; RW: AATCCAGTACTCGCCGCTCT), *mct1* (FW: TCATGTATGCTGGAGGACCAA; RW: AGTCG ACAAGAACACTGGGC), *mct4* (FW: AGACCCTAGG AGAGTTGAGCC; RW: CTCCATCCGGTGCTTTGAC T). For each sample, the relative expression level of each studied mRNA was normalized using *gapdh* (FW: AGTG TCAGGACGAACAGAGGCT; RW: GCCAATGCGACC GAATCCGTTA) as invariant control.

Reticulum fiber staining method

Slides were cut to 4 micron and stained with a silver impregnation-based kit for reticulin staining (Bio-Optica Bo 04-040,801, Milan, Italy). The staining steps were followed according to the manufacturer's instructions [46].

Statistical analysis

The data are expressed as mean \pm SD. Statistical analysis was carried out by Student's t-test, ANOVA test. A p -value < 0.05 was considered to indicate a statistically significant difference between experimental and control groups.

Results

Increased levels of circulating lactate sustain the expansion of immune suppressive subsets in MF patients

Lactate concentration was measured in PB sera from PMF ($n = 23$) compared to healthy matched controls (HC; $n = 16$). The amount of circulating lactate was significantly increased in sera from patients in comparison with HC (3.69 ± 2.2 vs. 1.08 ± 0.3 mmol/L, $p < 0.0001$; Fig. 1A).

Given that MPN patients exhibit immune alterations, including derangement of Treg and myeloid derived suppressor cells (MDSCs) [44, 47–49], we investigated the role of higher circulating lactate in promoting expansion of immunosuppressive subsets. After 48 h exposure of healthy PBMCs to medium conditioned with 20% sera from HC ($n = 10$) or PMF ($n = 16$), we found a significant increase of the percentage of both Treg and monocytic-MDSCs (M-MDSCs) in PBMCs cultured with PMF sera compared to the same cells grown with HC ones ($p < 0.001$; Fig. 1B, D). Of note, any significative difference was assessed by exposure of healthy PBMCs to media supplemented with FBS. To better define the role of lactate in the expansion of these immune suppressive subsets, we cultured PBMCs with PMF sera with or without

AZD3965, a selective inhibitor MCT1, to inhibit lactate import. The addition of AZD3965 decreased expansion of Treg and M-MDSCs of about $8.04 \pm 0.2\%$ and $6.98 \pm 6.2\%$ respectively ($p < 0.0001$ and $p = 0.0251$; Fig. 1C, E). Collectively these data demonstrate that increased circulating lactate contribute to immune deregulation observed in MF patients.

Lactate stimulates CAF phenotype and osteogenic differentiation in MSCs

A line of evidence suggests that lactate can activate a CAF phenotype in stromal cells sustaining formation of tumor niche [32, 36]. Therefore, we next evaluated the role of lactate in MSCs reprogramming by using an in vitro model of healthy MSCs (HS-5). The evaluation of CAF biomarkers expression after exposure to 20 mM lactate concentration unveiled a significant upregulation of alpha-smooth muscle actin (α SMA), platelet-derived growth factor receptor β (PDGFR β) and fibroblast activation protein alpha (FAP) and after 48 h ($p < 0.001$ and $p < 0.0001$ respectively; Fig. 2A). Notably, chronic exposure to high lactate also raised the concentration of osteoblast differentiation markers. In particular, after 10 days, lactate exposure increased the amount of BMP2, osteopontin, calcitonin and sRANKL (respectively $p < 0.0001$, $p < 0.01$, $p < 0.0001$ and $p < 0.0001$ vs. untreated cells; Fig. 2B), similarly to cells cultured in osteogenic induction medium (OIM). Alizarin red staining confirmed the increased deposition of calcium phosphate after chronic exposure to lactate (Fig. 2C); interestingly, this effect was reverted by AZD3965 treatment. Together, these results suggest that lactate-induced HS-5 cells toward a CAF-activated phenotype and chronic exposure of these cells to the metabolite stimulates osteogenic differentiation.

Lactate stimulates stromal cells to produce collagen favoring fibrotic transformation of TME

Given the significance of fibrotic tumor formation in MF patients, we next tested the role of high lactate concentration in promoting fibrosis. After 48 h lactate exposure, we found a significant upregulation of alpha-1 type I collagen (Col1A1; $p < 0.001$ vs. untreated cells; Fig. 3A). As showed in Fig. 3B, AZD3965 prevented lactate-induced Col1A1 expression ($p < 0.001$ vs. lactate treatment alone). Consistently, Mallory trichrome staining evidenced increased deposition of collagen in lactate treated stromal cells ($p < 0.01$ vs. untreated; Fig. 3C). Lactate-induced collagen deposition was partially reduced by MCT1 selective inhibitor AZD3965 ($p < 0.05$ vs. lactate treatment alone). These changes were sustained by a significant increase of key proteins involved in ECM degradation as MMP-2, MMP-9, RANTES and CHI3L1 (Fig. 3D). Expression of MMP-2 and RANTES raised already after 48 h lactate exposure (respectively $p < 0.0001$ and $p < 0.001$ vs.

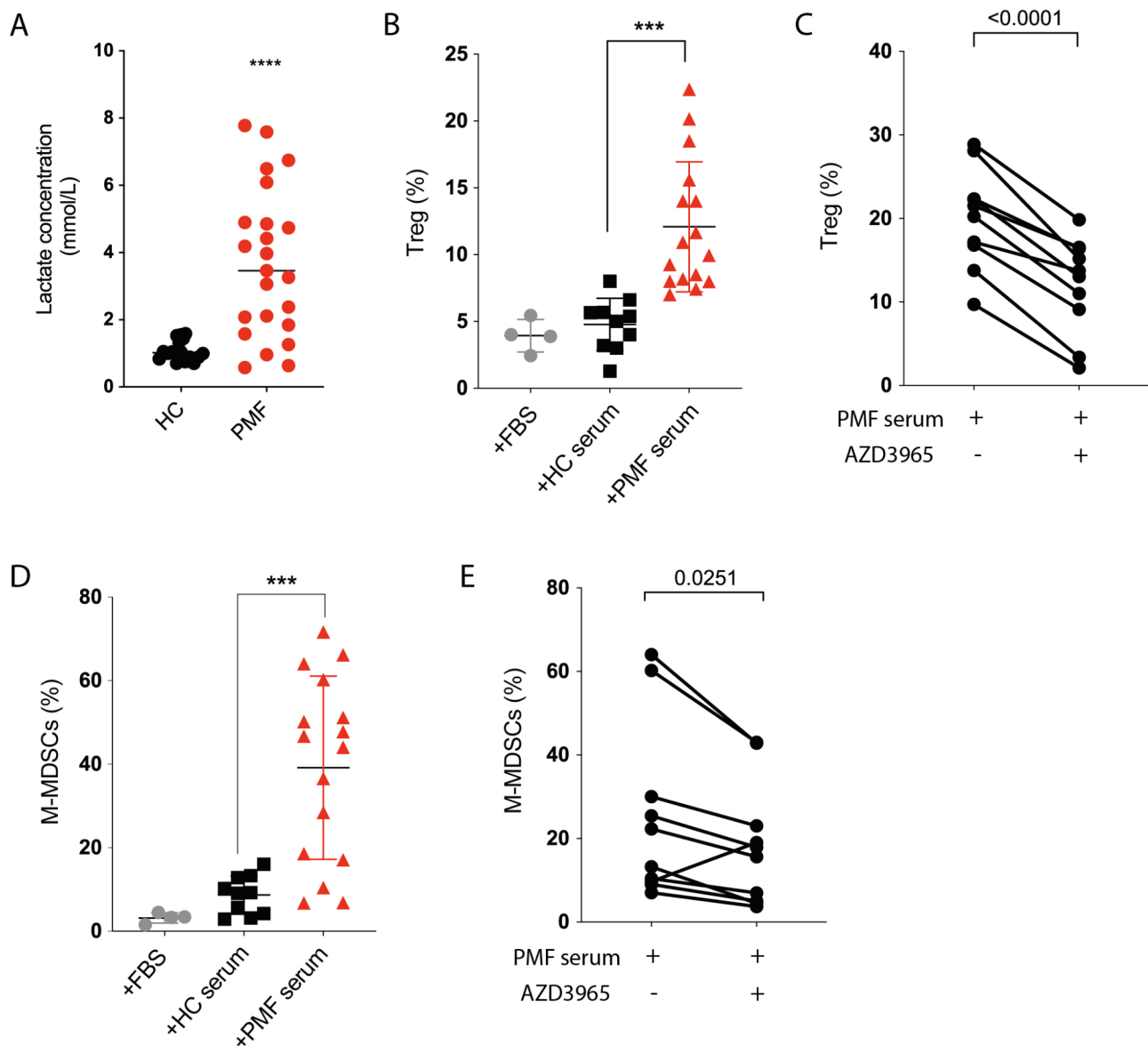


Fig. 1 High circulating lactate in MF sera favors immune deregulation. **(A)** Evaluation of Lactate concentration in PB from healthy and PMF patients. **(B)** Analysis of the percentage of Treg and **(D)** M-MDSCs after culturing healthy PBMCs with HC or PMF serum. **(C)** Evaluation of 10 μ M AZD3965 effects on circulating lactate-induced Treg and **(E)** M-MDSC expansion. Data are presented as means \pm SD. *** p < 0.001; **** p < 0.0001

untreated cells). To better elucidate the role of high circulating lactate in MF patients' sera in this context, we therefore compared the effect of healthy and PMF sera on collagen deposition. Following 24 h exposure to PMF sera, HS-5 cells showed a higher collagen accumulation compared to stromal cells treated with lactate (Fig. 3E). Of note, there was no significant increase when the culture medium was supplemented with healthy serum (Fig. 3E). Most importantly, the amount of collagen in cells treated with PMF sera or with lactate was similar after 48 h. Notably, PMF serum-induced collagen accumulation was inhibited by AZD3965 (p < 0.0001 vs. PMF serum condition; Fig. 3F). Collectively, these results

suggest that lactate increases collagen deposition in stromal cells contributing to ECM changes and fibrotic transformation of TME.

Alteration of lactate and its transporters in TPO^{high} zebrafish model

To further validate the in vitro data, we generated for the first time a thrombopoietin (TPO) high zebrafish model based on repeated exposure of supra-pharmacological doses of Eltrombopag Olamine for 15 days (Fig. 4A). TPO is the principal physiologic regulator of platelet production. Studies suggest that TPO mimetics promote

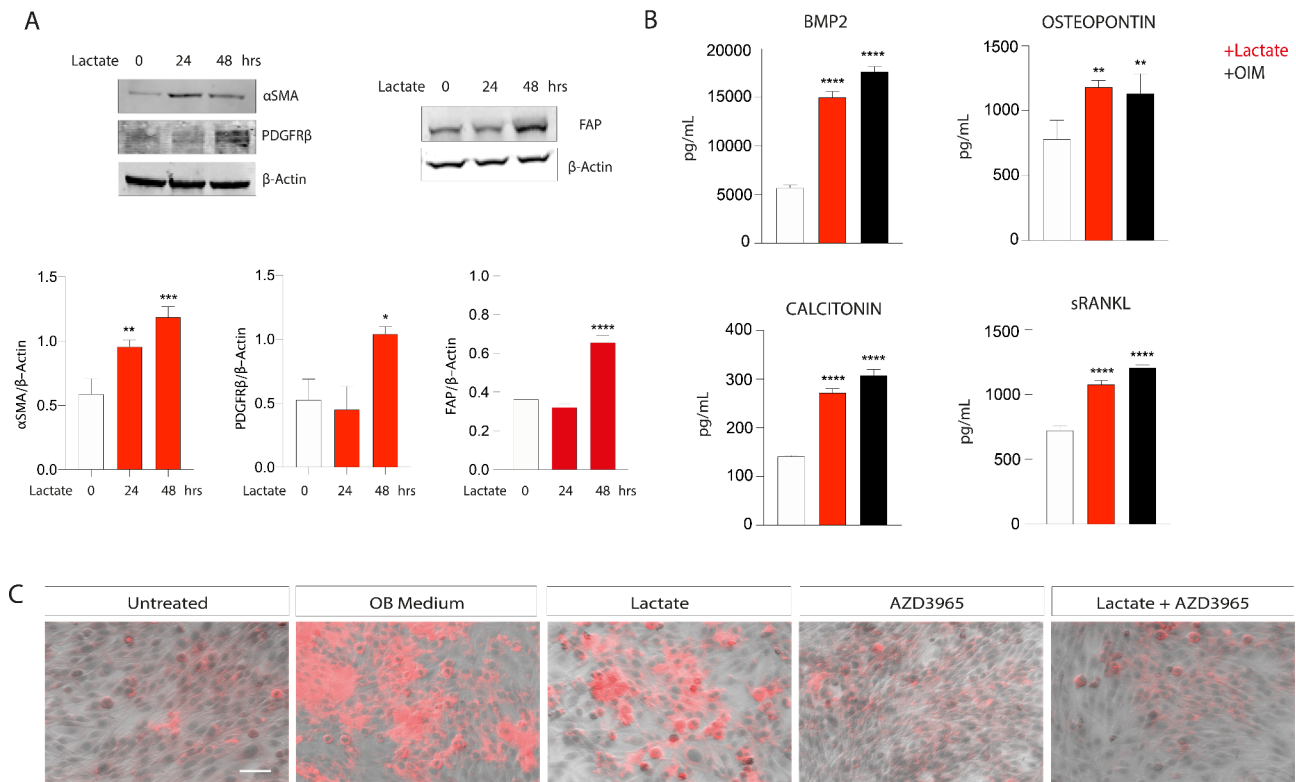


Fig. 2 Effect of lactate on stromal cell phenotype. **(A)** Cropped blots and densitometric analysis from western blot analysis on α SMA, PDGFR β and FAP, normalized on β -actin. **(B)** Multiplex immunobead assay technology on culture medium from HS5 cells after 10 days of 20 mM lactate exposure to determine concentrations of indicated osteoblast differentiation markers. **(C)** Alizarin red S staining for mineralization. The calcified nodules appeared bright red in color. Scale bar: 20 μ m. All the data are presented as means \pm SD of three independent experiments. * p < 0.05; ** p < 0.01; *** p < 0.001; **** p < 0.0001

reticulin deposition through stimulation of cytokine production by megakaryocytes, including TGF- β [50].

Analyzing the WKM, which is equivalent to the hematopoietic BM of mammals [45], the major blood lineages were measured using combined scatter profiles [39]. Therefore, we first evaluated the effect of TPO mimetic treatment on the distribution of several blood cells. As shown in Fig. 4B-C, we found an increased percentage of progenitor cells in TPO^{high} zebrafish ($n=9$) compared to controls ($n=5$) ($p < 0.01$); on the other hand, the number of erythroid and myeloid cells decreased significantly ($p < 0.001$ and $p < 0.01$ respectively). The increased number of precursors in TPO^{high} zebrafish was also confirmed by morphologic analysis of WKM (Fig. 4D). Moreover, TPO^{high} zebrafish showed a prominent upregulation of the megakaryocytic marker *cd41* and *mpl* ($p < 0.05$ compared to control; Fig. 4E) associated to a higher expression of *coll1a1* and *tgfb1* (respectively $p < 0.001$ and $p < 0.05$ vs. untreated group; Fig. 4F). Consistently with these results, TPO^{high} zebrafish displayed increased deposition of *Coll1a1* and reticulum fibers in WKM suggesting establishment of fibrosis (Fig. 4G-H). Notably, levels of lactate in the WKM were higher in TPO^{high} zebrafish compared to untreated animals ($p < 0.05$; Fig. 5A). Moreover, the analysis of lactate transporters

expression unveiled a significant upregulation of *mct1* accompanied by a strong decrease of *mct4* expression ($p < 0.001$ compared to control; Fig. 5B), also confirmed by immunofluorescence (Fig. 5C). Taken together, these results demonstrated that lactate and its transporters are skewed in TPO^{high} zebrafish.

MCTs expression in PMF patients

To validate MCT4 downregulation in myelofibrosis, we analyzed MCT expression in BM biopsies from PMF patients. Immunohistochemical analysis of three consecutive slides revealed that PMF-MSCs, identified as CD90⁺ cells, expressed only MCT1 (Fig. 6A). Interestingly, evaluating expression of MCTs in PV, TE and PMF, we found that the loss of MCT4 is an exclusive feature of myelofibrosis TME (Fig. 6B).

Discussion

The evolution of MF is associated with the development of BM fibrosis, progressive splenomegaly and systemic symptoms. Concomitantly, metabolic alterations, occurring in cancer cells reshape TME through exchange of signaling molecules including metabolites which induce cancer-associated transformation and immune-escape [20, 51, 52]. Although metabolic alterations in MPN

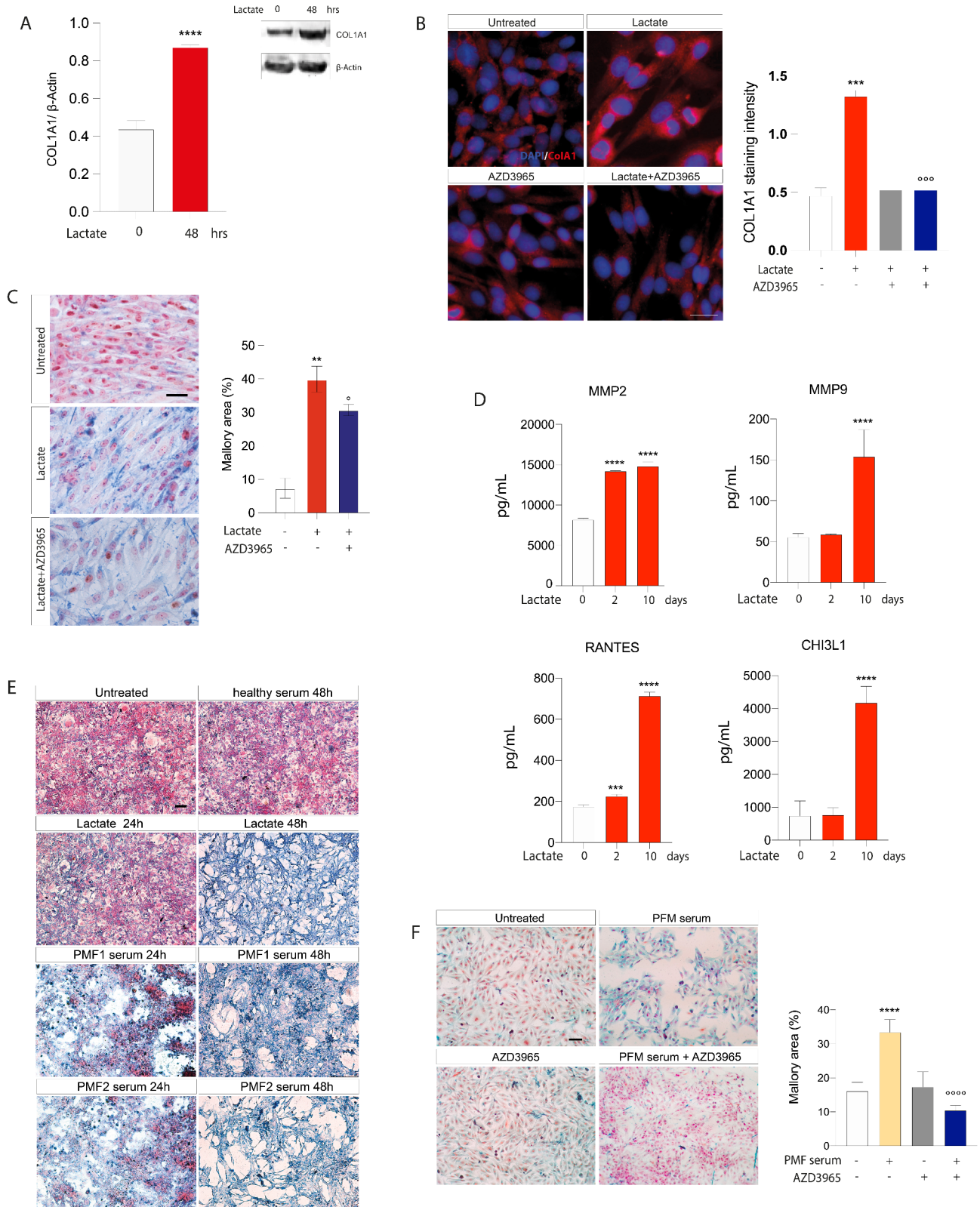


Fig. 3 (See legend on next page.)

(See figure on previous page.)

Fig. 3 HS5 cells increase collagen deposition after exposure to lactate. **(A)** Western blot analysis of COL1A1 protein after 20 mM lactate exposure. β -Actin protein was used as total protein loading reference. The optical density of the bands was measured using Scion Image software. **(B)** Representative pictures of COL1A1 staining in HS5 cells cultured in presence of 20 mM lactate and/or 10 μ M AZD3965. Scale bar: 20 μ m. Quantification of the protein intensity was calculated and graphed. **(C)** Evaluation of collagen fibers in HS5 cells after exposure to 20 mM lactate in presence or absence of MCT1 inhibitor for 48 h. Scale bar: 20 μ m. Magnification: 40X. Quantification of the Mallory area was calculated and graphed. **(D)** Multiplex immunobead assay technology on culture medium from HS5 cells after 2 and 10 days of 20 mM lactate exposure to determine concentrations of indicated proteins. **(E)** Mallory trichrome staining in HS5 after exposure to healthy or PMF sera. Scale bar: 100 μ m; magnification: 10X. **(F)** PMF serum with or without 10 μ M AZD3965. Quantification of the Mallory area was calculated and graphed. Scale bar: 20 μ m; magnification: 20X. All the data are presented as means \pm SD of three independent experiments. ** $p < 0.01$, *** $p < 0.001$, **** $p < 0.0001$ versus untreated; $^{\circ}p < 0.05$ and $^{\circ\circ}p < 0.001$ versus lactate alone; $^{\circ\circ\circ}p < 0.0001$ versus PMF serum

tumor cells have been previously described, insights on how these changes impact TME are poorly understood. In this study, we found an increased amount of circulating lactate in sera from myelofibrosis patients. These data are in accordance with previous works demonstrating an increased glycolytic rate in JAK2-V617F mutant cells [26, 28] and higher lactate levels in platelets from MPN patients [53]. Lactate deeply modulates immune response through the expansion of immunosuppressive subsets [20], prompting naïve T cell apoptosis [54] and decreasing the cytotoxic activity of NK [55]. We found that the exposure of healthy PBMCs to PMF sera induces the expansion of Treg and M-MDSC immunosuppressive subtypes. This effect is in part lactate-mediated as demonstrated by the significant reduction of the percentage of Treg and M-MDSCs after MCT1 blocking.

The pathophysiology underlying BM fibrosis remains unclear despite intensive study, with lack of specific therapy [56]. It is the outcome of complex interactions between myelofibrosis tumor cells and stromal cells, which, after differentiation into myofibroblasts and fibroblasts, lay down specific classes of collagen and matrix protein, culminating in the fibrotic transformation of the BM niche [13]. Lactate metabolism alterations have been noted in Idiopathic Pulmonary Fibrosis [42] and liver fibrosis [57], but the relationship between lactate and BM fibrosis has not been elucidated. Here, we demonstrated that lactate confers CAF phenotypic features to healthy MSCs, as suggested by increased α SMA and FAP expression after lactate exposure. It is generally accepted that CAFs are the main participants in ECM remodeling and fibrosis [58]. Furthermore, lactate has been reported to promote TGF- β signaling, eventually triggering tumor fibrosis [59]. Interestingly, our data demonstrated that lactate-induced CAFs engage in the release of osteo-inductive growth factors including BMP2, osteopontin, calcitonin and sRANKL, which leads to mineralized matrix formation. Pharmacological inhibition of MCT1 by AZD3965 prevented osteoblast differentiation. Osteoblasts dysregulation might cause secretion of large amounts of type I collagen and ECM remodeling, culminating in a stiff, type I collagen-rich fibrotic matrix [60]. After lactate exposure, HS-5 cells showed increased expression of COL1A1 and collagen accumulation which decreased after MCT1 inhibition. This lactate-induced

early fibrosis development was corroborated by higher secretion of MMP2, MMP9, RANTES and CHI3L1. As a proof of context, when excessive remodeling of ECM occurs, both the quantity of collagen and levels of MMPs increase significantly [61]. In this context, MMP-9 is highly expressed during fibrosis process, and it has become a research focus to reduce ECM deposition and inhibit fibrosis [62]. Notably, PMF serum lactate causes a strong deposition of collagen which was not observed after incubation of stromal cells with serum from healthy controls. This circulating lactate-induced effect was significantly reverted after addition of AZD3965.

We also performed a detailed analysis of lactate amount and its transporter expression in WKM from adult zebrafish after establishing experimental fibrosis. Indeed, this study provides evidence that, after treatment with a TPO mimetic, zebrafish become prone to develop fibrosis in WKM, the site for hematopoiesis in adult zebrafish [63]. This is in keeping with the TPO^{high} murine model known to recreate the phenotype of BM fibrosis shared by MF patients associated with increased megakaryocytes and splenomegaly [56, 64, 65]. After its binding to MPL receptor, TPO regulates megakaryopoiesis and induces proliferation of progenitor hematopoietic cells [50]. Moreover, thrombopoietin receptor agonists are reported to increase the risk for reticulin fiber deposition within bone marrow [66]. Consistently, TPO^{high} zebrafish showed higher expression of megakaryocyte-related and fibrosis-related genes, which was corroborated by increased deposition of collagen and reticulum fibers in WKM. Performing a detailed analysis of the major blood lineages, we also found higher number of progenitor cells accompanied by a reduction of erythroid and myeloid cells. Besides, we unveil a remarkable increase in lactate concentration accompanied by a higher expression of MCT1 and a strong downregulation of MCT4 in WKM from TPO^{high} zebrafish. To definitively unravel the expression of MCTs in myelofibrosis TME, we exploited their expression in biopsy specimens from MPN patients. Notably, our results demonstrate that, among the MPNs, myelofibrosis is the only characterized by the loss of MCT4 expression. It is well known that MCTs are the most important elements in lactate metabolism, orchestrating metabolic remodeling of TME. As MCT4 mediates lactate export in highly glycolytic cells

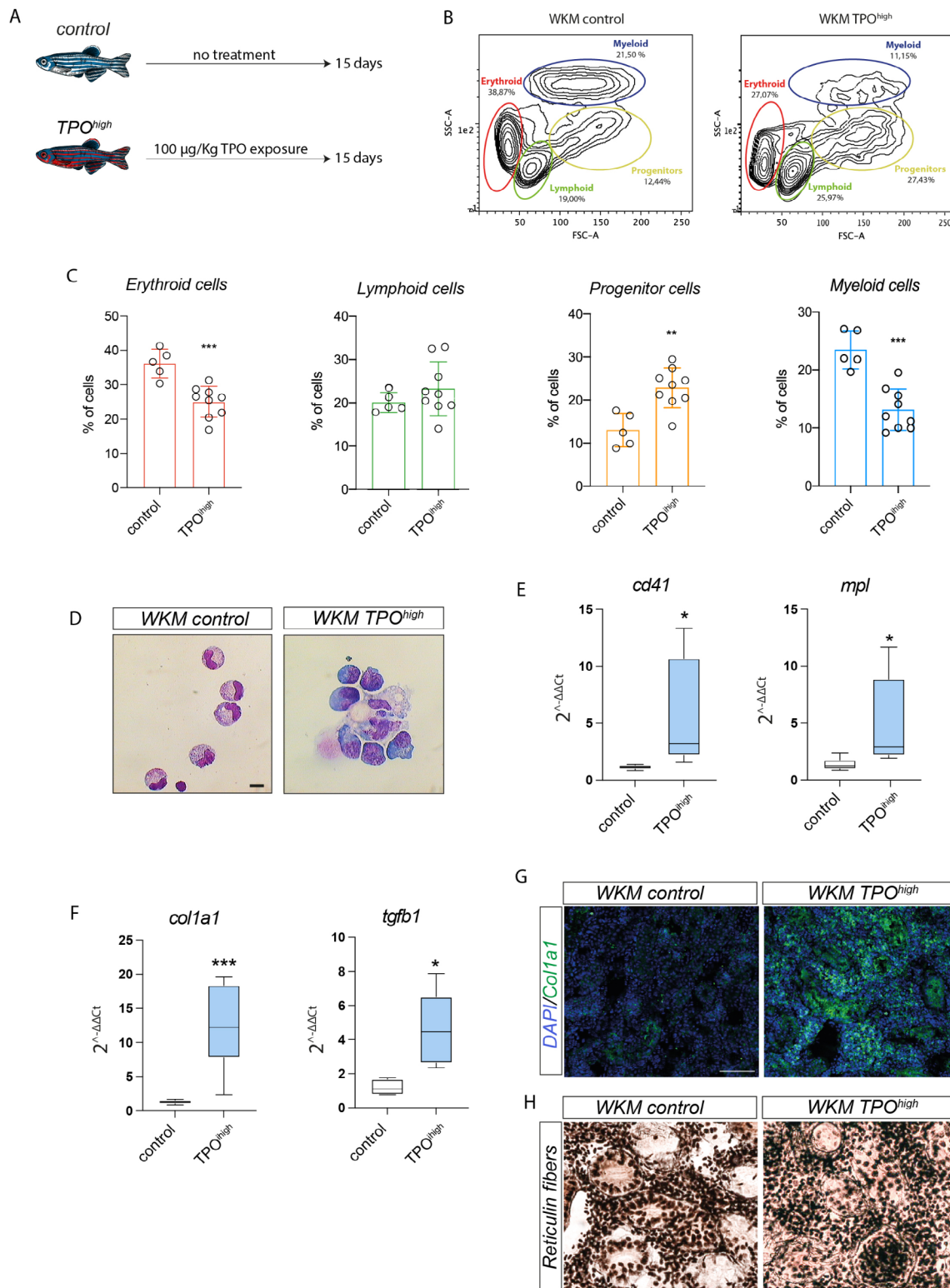


Fig. 4 TPO^{high} zebrafish as an in vivo model of megakaryocyte expansion and fibrosis development. **(A)** A schematic view of TPO^{high} zebrafish model. **(B)** Flow cytometry analysis of WKM in control and TPO^{high} zebrafish. **(C)** Evaluation of the percentage of each blood lineage after TPO treatment. **(D)** May-Grünwald Giemsa images of hematopoietic cells isolated from WKM of control and TPO^{high} zebrafish. Scale bar: 5 µm. **(E)** qPCR analysis of megakaryocytic markers and **(F)** *col1a1* and *tgfb1* expression in WKM. B2m was used as housekeeping gene. Calculated value of 2^{-ΔΔCt} in control was 1. **(G)** Representative immunofluorescence images of Col1A1 and **(H)** immunohistochemical images of reticulin fibers in control and TPO^{high} zebrafish. Scale bar: 40 µm; magnification: 40X. **p* < 0.05; ***p* < 0.01; ****p* < 0.001

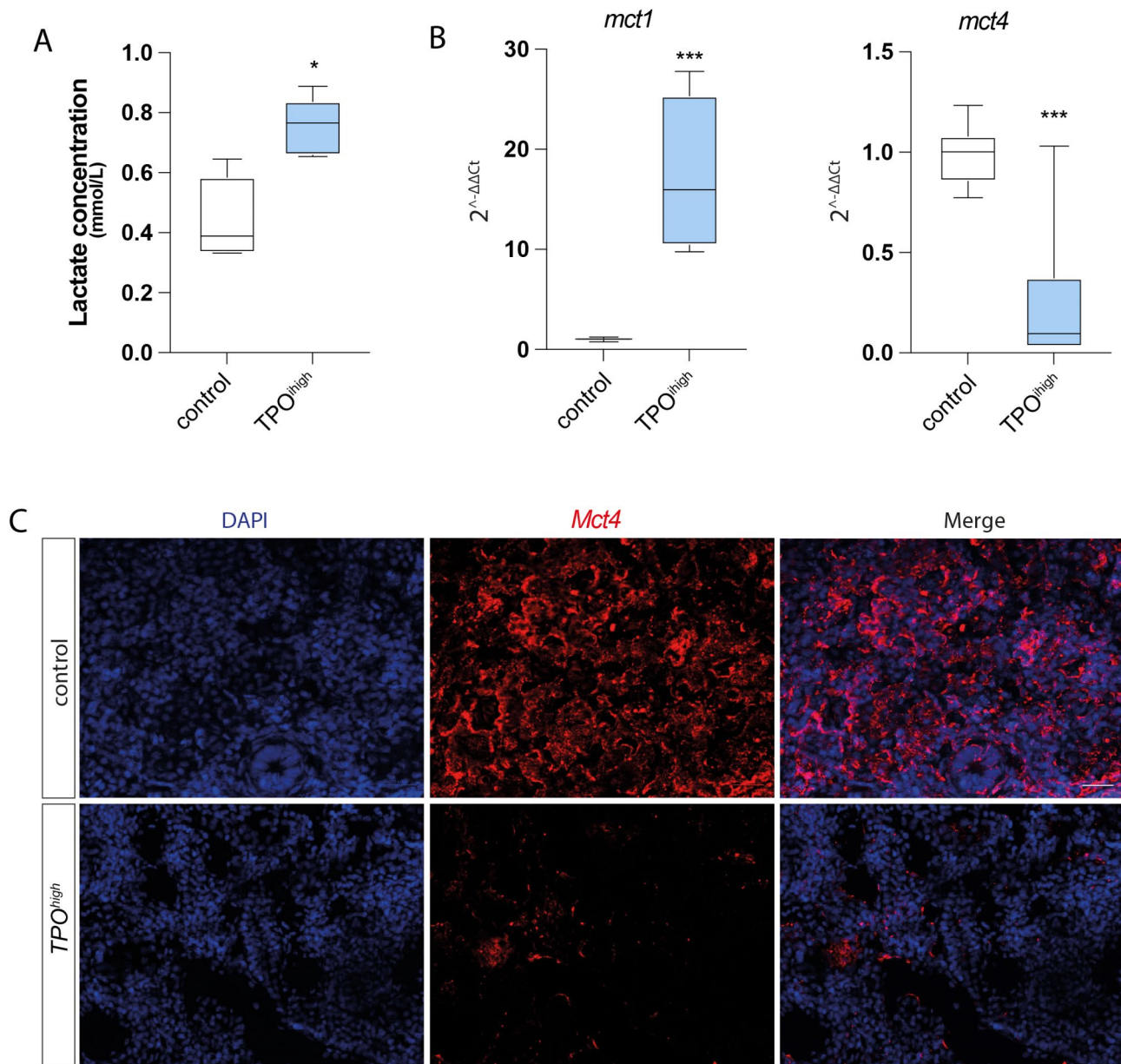


Fig. 5 Alteration of lactate and its transporters in TPO^{high} zebrafish model. **(A)** Evaluation of lactate concentration in WKM from control and TPO^{high} zebrafish. **(B)** qPCR analysis of *mct1* and *mct4* in WKM from control and TPO^{high} animals. **(C)** Representative immunofluorescence images for Mct4. Scale bar: 20 μ m. All the data are presented as means \pm SD of three independent experiments. * $p < 0.05$; *** $p < 0.001$

[67, 68], a deeply metabolic adaptation may occur in MF patients. Most importantly, the heterogeneity of MCT1, which is expressed in different cell populations, and the homogeneity loss of MCT4 expression in PMF biopsies might contribute to lactate accumulation in BM, supporting tumor fibrosis and progression. Further studies will be developed in order to investigate the potential role of MCT4 as a potential marker of clinical utility in the differential diagnosis between TE and early stage of myelofibrosis.

Conclusions

In conclusion, our results unveil lactate as a key regulator of immune escape and BM fibrotic transformation in MF patients, reinforcing the idea that targeting metabolism can be a good strategy against cancer. Moreover, our data represent the first experimental evidence of a BM fibrotic phenotype in TPO^{high} zebrafish model, together with several hematological features of the disease observed in MF patients. Our results suggest that changes in MCT expression in TME is an effect occurring during fibrosis development, despite a causal link between the loss of MCT4 and pro-fibrotic phenotype needs to

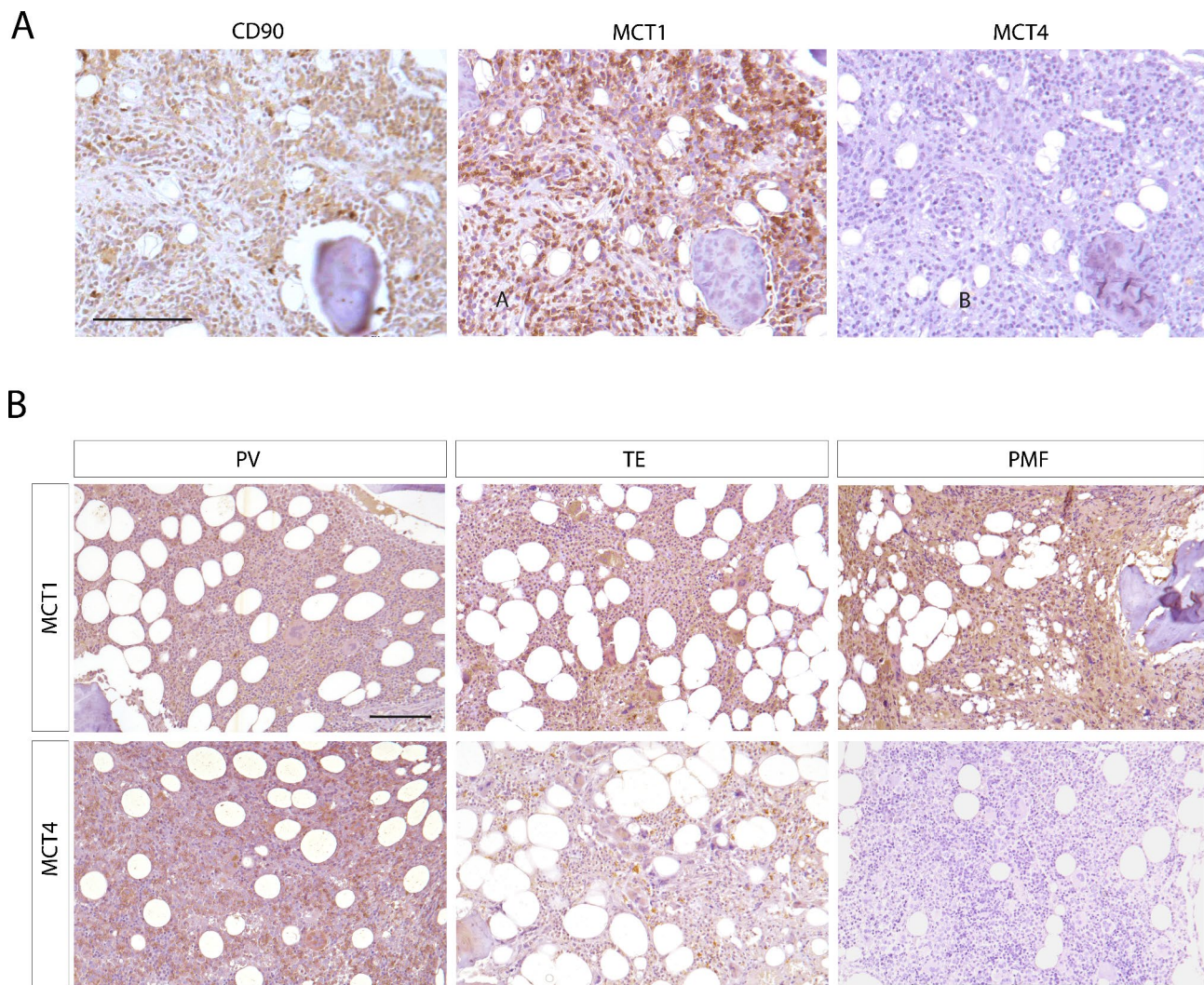


Fig. 6 MCTs expression in BM biopsies from MPN patients. **(A)** Immunohistochemical analysis of CD90, MCT1 and MCT4 expression in three consecutive sections from a PMF BM biopsy. **(B)** Representative immunohistochemical images of MCT1 and MCT4 in BM slides from PV, TE and PMF patients. Scale bar: 500 px

be demonstrated. To date, identifying novel antifibrotic strategies is very important since the effectiveness of current therapies in reverting BM fibrosis is debated. Our results demonstrate that MCT1 might be a novel druggable target in MF paving the way to antifibrotic therapies based on the inhibition of lactate accumulation in tumor microenvironment.

Abbreviations

αSMA	Alpha-smooth muscle actin
BM	Bone marrow
BMP2	Bone morphogenetic protein 2
CAF	Cancer-associated phenotype
CHI3L1	Chitinase 3 like 1
Col1A1	Alpha-1 type I collagen
ECM	Extracellular matrix
ET	Essential thrombocythemia
FAP	Fibroblast activation protein alpha
JAKi	JAK inhibitors
LDHA	Lactate dehydrogenase A

MCTs	Monocarboxylate transporters
MDSCs	Myeloid derived suppressor cells
MF	Myelofibrosis
MMPs	Matrix metallopeptidases
MPN	Myeloproliferative neoplasm
MSCs	Mesenchymal stromal cells
OIM	Osteogenic induction medium
PB	Peripheral blood
PBMCs	Peripheral blood mononuclear cells
PDGFRβ	Platelet-derived growth factor receptor β
PMF	Primary myelofibrosis
PV	Polycythemia vera
RANTES/CCL5	Regulated upon activation, normal T cell expressed and secreted
sRANKL	Receptor activator of nuclear factor kappa-B ligand
TGF-β	Tumor growth factor beta
TME	Tumor microenvironment
TPO	Thrombopoietin
WKM	Whole kidney marrow

Supplementary Information

The online version contains supplementary material available at <https://doi.org/10.1186/s12967-025-06083-4>.

Supplementary Material 1

Acknowledgements

This study has been supported in part by A.I.L. (Associazione Italiana contro le Leucemie) sezione di Catania and by FON.CA.NE.SA. (Fondazione Catanese per lo Studio delle Malattie Neoplastiche del Sangue).

Author contributions

Conceptualization: DT, CG, GAP and GLV; project administration: DT, CG, GAP, FDR, SG and GLV; methodology: MS, CG, ELS, AD, LL, RC, LS, ID, GB, VDF and AR; investigation: MS, CG, ELS, AD, LL, RC, LS, GB, AMDM, VDF and AR; formal analysis: CG, SG, DT, GAP, FDR and GLV; resources: MS, CG, SG, DT, GAP and GLV; supervision: CG, GAP, DT and GLV; writing-original draft: CG, SG, GAP, EPP, DT and GLV; writing-reviewing and editing: FDR, AR, RC, CG, SG, GAP, DT and GLV.

Funding

This work was founded by the PRIN 2022 project entitled "The biochemical and clinical significance of lactate metabolism in patients with myelofibrosis: a new target to improve the clinical outcome", project code 2022C4x4W4, proposals D.D. n. 104 of 2 February 2022 M4C211.1 funded by the European Union – NextGenerationEU.

Data availability

The datasets used and/or analyzed in this study are reported within the manuscript and/or additional files and are available from the corresponding authors.

Declarations

Ethics approval and consent to participate

Peripheral blood (PB) samples were collected from MF patients and age-matched controls after written informed consent (Azienda Ospedaliero-Universitaria Policlinico "G.Rodolico-San Marco", n. 54/2022/PO).

Consent for publication

Not applicable.

Competing interests

The authors declare no conflict of interest.

Author details

¹Department of Biomedical and Biotechnological Sciences, Division of Medical Biochemistry, University of Catania, Catania, Italy

²Department of Medical and Surgical Sciences and Advanced Technologies "G.F. Ingrassia", Division of Hematology, University of Catania, Catania, Italy

³Hematology Unit with BMT, A.O.U. Policlinico "G. Rodolico-San Marco", Catania, Italy

⁴Department of Medical and Surgical Sciences and Advanced Technologies "G.F. Ingrassia", Division of Anatomic Pathology, University of Catania, Catania, Italy

⁵Anatomic Pathology, A.O.U. Policlinico "G. Rodolico-San Marco", Catania, Italy

⁶Department of Clinical and Experimental Medicine, University of Catania, Catania, Italy

⁷Ospedale Cannizzaro, Catania, Italy

⁸Department of General Surgery and Medical-Surgical Specialties, University of Catania, Catania, Italy

Received: 5 November 2024 / Accepted: 6 January 2025

Published online: 14 January 2025

References

- Longhitano L, Li Volti G, Giallongo C, Spampinato M, Barbagallo I, Di Rosa M, Romano A, Avola R, Tibullo D, Palumbo GA. The role of inflammation and inflammasome in Myeloproliferative disease. *J Clin Med*. 2020;9(8).
- Duminuco A, Torre E, Palumbo GA, Harrison C. A journey through JAK inhibitors for the treatment of Myeloproliferative diseases. *Curr Hematol Malig Rep*. 2023;18(5):176–89.
- Song Z, Liu X, Zhang W, Luo Y, Xiao H, Liu Y, Dai G, Hong J, Li A. Ruxolitinib suppresses liver fibrosis progression and accelerates fibrosis reversal via selectively targeting Janus kinase 1/2. *J Transl Med*. 2022;20(1):157.
- Greenfield G, McPherson S, Mills K, McMullin MF. The ruxolitinib effect: understanding how molecular pathogenesis and epigenetic dysregulation impact therapeutic efficacy in myeloproliferative neoplasms. *J Transl Med*. 2018;16(1):360.
- Duminuco A, Nardo A, Giuffrida G, Leotta S, Markovic U, Giallongo C, Tibullo D, Romano A, Di Raimondo F, Palumbo GA. Myelofibrosis and survival prognostic models: a journey between past and future. *J Clin Med*. 2023;12(6).
- Zhu P, Lai X, Liu L, Shi J, Yu J, Zhao Y, Yang L, Yang T, Zheng W, Sun J, Wu W, Zhao Y, Cai Z, Huang H, Luo Y. Impact of myelofibrosis on patients with myelodysplastic syndromes following allogeneic hematopoietic stem cell transplantation. *J Transl Med*. 2024;22(1):275.
- Duminuco A, Chifotides HT, Giallongo S, Giallongo C, Tibullo D, Palumbo GA. ACVR1: a novel therapeutic target to treat anemia in myelofibrosis. *Cancers (Basel)*. 2023;16(1).
- Duminuco A, Vetro C, Giallongo C, Palumbo GA. The pharmacotherapeutic management of patients with myelofibrosis: looking beyond JAK inhibitors. *Expert Opin Pharmacother*. 2023;24(13):1449–61.
- Tefferi A. Primary myelofibrosis. 2017 update on diagnosis, risk-stratification, and management. *Am J Hematol*. 2016;91(12):1262–71.
- Giallongo S, Duminuco A, Dulcamare I, Zuppelli T, La Spina E, Scandura G, Santisi A, Romano A, Di Raimondo F, Tibullo D, Palumbo GA, Giallongo C. Engagement of Mesenchymal stromal cells in the remodeling of the bone marrow microenvironment in hematological cancers. *Biomolecules*. 2023;13(12).
- Jamieson C, Hasserjian R, Gotlib J, Cortes J, Stone R, Talpaz M, Thiele J, Rodig S, Pozdnyakova O. Effect of treatment with a JAK2-selective inhibitor, fedratinib, on bone marrow fibrosis in patients with myelofibrosis. *J Transl Med*. 2015;13:294.
- Spampinato M, Giallongo C, Romano A, Longhitano L, La Spina E, Avola R, Scandura G, Dulcamare I, Bramanti V, Di Rosa M, Vicario N, Parenti R, Li Volti G, Tibullo D. G.A. Palumbo. Focus on osteosclerotic progression in primary Myelofibrosis. *Biomolecules*. 2021;11(1).
- Ghosh K, Shome DK, Kulkarni B, Ghosh MK, Ghosh K. Fibrosis and bone marrow: understanding causation and pathobiology. *J Transl Med*. 2023;21(1):703.
- Schneider RK, Ziegler S, Leisten I, Ferreira MS, Schumacher A, Rath B, Fahrenkamp D, Muller-Newen G, Crysandt M, Wilop S, Jost E, Koschmieder S, Knuchel R, Brummendorf TH, Ziegler P. Activated fibronectin-secretory phenotype of mesenchymal stromal cells in pre-fibrotic myeloproliferative neoplasms. *J Hematol Oncol*. 2014;7:92.
- Leimkuhler NB, Gleitz HFE, Ronghui L, Snoeren IAM, Fuchs SNR, Nagai JS, Banjanin B, Lam KH, Vogl T, Kuppe C, Stalman USA, Busche G, Kreipe H, Gutgemann I, Krebs P, Banz Y, Boor P, Tai EW, Brummendorf TH, Koschmieder S, Crysandt M, Bindels E, Kramann R, Costa IG, Schneider RK. Heterogeneous bone-marrow stromal progenitors drive myelofibrosis via a druggable alarmin axis. *Cell Stem Cell*. 2021;28(4):637–e6528.
- Martinaud C, Desterke C, Konopacki J, Pieri L, Torossian F, Golub R, Schmutz S, Anginot A, Guerton B, Rochet N, Albanese P, Henault E, Pierre-Louis O, Souraud JB, de Revel T, Dupriez B, Ianotto JC, Bourgeade MF, Vannucchi AM, Lataillade JJ. Le Bousse-Kerdiles, osteogenic potential of mesenchymal stromal cells contributes to primary myelofibrosis. *Cancer Res*. 2015;75(22):4753–65.
- Pavlova NN, Thompson CB. The emerging Hallmarks of Cancer Metabolism. *Cell Metab*. 2016;23(1):27–47.
- Duan SL, Wu M, Zhang ZJ, Chang S. The potential role of reprogrammed glucose metabolism: an emerging actionable codependent target in thyroid cancer. *J Transl Med*. 2023;21(1):735.
- Brierley CK, Psaila B. Sugar thieves and addicts: nutrient subversion in JAK2 MPNs. *Blood*. 2019;134(21):1778–80.
- Barbato A, Giallongo C, Giallongo S, Romano A, Scandura G, Concetta S, Zuppelli T, Lolicato M, Lazzarino G, Parrinello N, Del Fabro V, Fontana P, Aguenno M, Li G, Volti GA, Palumbo F, Di Raimondo D, Tibullo. Lactate

- trafficking inhibition restores sensitivity to proteasome inhibitors and orchestrates immuno-microenvironment in multiple myeloma. *Cell Prolif.* 2023;56(4):e13388.
21. Xie J, Wu H, Dai C, Pan Q, Ding Z, Hu D, Ji B, Luo Y, Hu X. Beyond Warburg effect—dual metabolic nature of cancer cells. *Sci Rep.* 2014;4:4927.
 22. Jang M, Kim SS, Lee J. Cancer cell metabolism: implications for therapeutic targets. *Exp Mol Med.* 2013;45(10):e45.
 23. Sharma D, Singh M, Rani R. Role of LDH in tumor glycolysis: regulation of LDHA by small molecules for cancer therapeutics. *Semin Cancer Biol.* 2022;87:184–95.
 24. Longhitano L, Vicario N, Tibullo D, Giallongo C, Broggi G, Caltabiano R, Barbagallo GMV, Altieri R, Baghini M, Di Rosa M, Parenti R, Giordano A, Mione MC. Li Volti, Lactate induces the expressions of MCT1 and HCAR1 to promote Tumor Growth and Progression in Glioblastoma. *Front Oncol.* 2022;12:871798.
 25. Shah S, Mudreddy M, Hanson CA, Ketterling RP, Gangat N, Pardanani A, Tefferi A. Marked elevation of serum lactate dehydrogenase in primary myelofibrosis: clinical and prognostic correlates. *Blood Cancer J.* 2017;7(12):657.
 26. Reddy MM, Fernandes MS, Deshpande A, Weisberg E, Inguiluzin HV, Abdel-Wahab O, Kung AL, Levine RL, Griffin JD, Sattler M. The JAK2V617F oncogene requires expression of inducible phosphofructokinase/fructose-bisphosphatase 3 for cell growth and increased metabolic activity. *Leukemia.* 2012;26(3):481–9.
 27. Yi M, Ban Y, Tan Y, Xiong W, Li G, Xiang B. 6-Phosphofructo-2-kinase/fructose-2,6-bisphosphatase 3 and 4: a pair of valves for fine-tuning of glucose metabolism in human cancer. *Mol Metab.* 2019;20:1–13.
 28. Rao TN, Hansen N, Hilfiker J, Rai S, Majewska JM, Lekovic D, Gezer D, Andina N, Galli S, Cassel T, Geier F, Delezio J, Nienhold R, Hao-Shen H, Beisel C, Di Palma S, Dimeloe S, Trebicka J, Wolf D, Gassmann M, Fan TW, Lane AN, Handschin C, Dirnhofer S, Kroger N, Hess C, Radimerski T, Koschmieder S, Cokic VP, Skoda RC. JAK2-mutant hematopoietic cells display metabolic alterations that can be targeted to treat myeloproliferative neoplasms. *Blood.* 2019;134(21):1832–46.
 29. Longhitano L, Vicario N, Forte S, Giallongo C, Broggi G, Caltabiano R, Barbagallo GMV, Altieri R, Raciti G, Di Rosa M, Caruso M, Parenti R, Liso A, Busi F, Lolicato M, Mione MC, Li G, Volti D, Tibullo. Lactate modulates microglia polarization via IGFBP6 expression and remodels tumor microenvironment in glioblastoma. *Cancer Immunol Immunother.* 2023;72(1):1–20.
 30. Ishihara S, Hata K, Hirose K, Okui T, Toyosawa S, Uzawa N, Nishimura R, Yoneda T. The lactate sensor GPR81 regulates glycolysis and tumor growth of breast cancer. *Sci Rep.* 2022;12(1):6261.
 31. Sangsuwan R, Thuamsang B, Pacifici N, Allen R, Han H, Miakicheva S, Lewis JS. Lactate exposure promotes immunosuppressive phenotypes in Innate Immune cells. *Cell Mol Bioeng.* 2020;13(5):541–57.
 32. Linares JF, Cid-Diaz T, Duran A, Osrodek M, Martinez-Ordenez A, Reina-Campos M, Kuo HH, Elemento O, Martin ML, Cordes T, Thompson TC, Metallo CM, Moscat J. Diaz-Meco, the lactate-NAD(+) axis activates cancer-associated fibroblasts by downregulating p62. *Cell Rep.* 2022;39(6):110792.
 33. Sun Z, Ji Z, Meng H, He W, Li B, Pan X, Zhou Y, Yu G. Lactate facilitated mitochondrial fission-derived ROS to promote pulmonary fibrosis via ERK/DRP-1 signaling. *J Transl Med.* 2024;22(1):479.
 34. Hu S, Ye J, Guo Q, Zou S, Zhang W, Zhang D, Zhang Y, Wang S, Su L, Wei Y. Serum lactate dehydrogenase is associated with impaired lung function: NHANES 2011–2012. *PLoS ONE.* 2023;18(2):e0281203.
 35. Kottmann RM, Kulkarni AA, Smolnycki KA, Lyda E, Dahanayake T, Salibi R, Honnons S, Jones C, Isern NG, Hu JZ, Nathan SD, Grant G, Phipps RP, Sime PJ. Lactic acid is elevated in idiopathic pulmonary fibrosis and induces myofibroblast differentiation via pH-dependent activation of transforming growth factor-beta. *Am J Respir Crit Care Med.* 2012;186(8):740–51.
 36. Kitamura F, Semba T, Yasuda-Yoshihara N, Yamada K, Nishimura A, Yamasaki J, Nagano O, Yasuda T, Yonemura A, Tong Y, Wang H, Akiyama T, Matsumura K, Uemura N, Itoyama R, Bu L, Fu L, Hu X, Wei F, Mima K, Imai K, Hayashi H, Yamashita YI, Miyamoto Y, Baba H, Ishimoto T. Cancer-associated fibroblasts reuse cancer-derived lactate to maintain a fibrotic and immunosuppressive microenvironment in pancreatic cancer. *JCI Insight.* 2023;8(20).
 37. Li D, Wang M, Fan R, Song Z, Li Z, Gan H, Fan H. Clusterin regulates TRPM2 to protect against myocardial injury induced by acute myocardial infarction injury. *Tissue Cell.* 2023;82:102038.
 38. Kanehara A, Kotake R, Miyamoto Y, Kumakura Y, Morita K, Ishiura T, Shimizu K, Fujieda Y, Ando S, Kondo S, Kasai K. Correction to: the Japanese version of the questionnaire about the process of recovery: development and validity and reliability testing. *BMC Psychiatry.* 2020;20(1):12.
 39. Traver D, Paw BH, Poss KD, Penberthy WT, Lin S, Zon LI. Transplantation and in vivo imaging of multilineage engraftment in zebrafish bloodless mutants. *Nat Immunol.* 2003;4(12):1238–46.
 40. Romano A, Parrinello NL, Vetro C, Tibullo D, Giallongo C, La Cava P, Chiarenza A, Motta G, Caruso AL, Villari L, Tripodo C, Cosentino S, Ippolito M, Consoli U, Gallamini A, Pileri S. Di Raimondo, the prognostic value of the myeloid-mediated immunosuppression marker Arginase-1 in classic Hodgkin lymphoma. *Oncotarget.* 2016;7(41):67333–46.
 41. Giallongo S, Rehakova D, Biagini T, Lo Re O, Raina P, Lochmanova G, Zdrahal Z, Resnick I, Pata P, Pata I, Mistrik M, de Magalhaes JP, Mazza T, Koutna I, Vinciguerra M. Histone variant macroH2A1.1 enhances nonhomologous end joining-dependent DNA double-strand-break repair and reprogramming efficiency of human iPSCs. *Stem Cells.* 2022;40(1):35–48.
 42. Longhitano L, Distefano A, Musso N, Bonacci P, Orlando L, Giallongo S, Tibullo D, Denaro S, Lazzarino G, Ferrigno J, Nicolosi A, Alanazi AM, Salomone F, Tropea E, Barbagallo IA, Bramanti V, Li Volti G, Lazzarino G, Torella D, Amorini, (+)-Lipoic acid reduces mitochondrial unfolded protein response and attenuates oxidative stress and aging in an in vitro model of non-alcoholic fatty liver disease. *J Transl Med.* 2024;22(1):82.
 43. Wolun-Cholewa M, Szymanowski K, Andrusiewicz M, Szczerba A, Warchoł JB. Trichrome Mallory's stain may indicate differential rates of RNA synthesis in eutopic and ectopic endometrium. *Folia Histochem Cytobiol.* 2010;48(1):148–52.
 44. Veletic I, Prijic S, Manshouri T, Noguera-Gonzalez GM, Verstovsek S, Estrov Z. Altered T-cell subset repertoire affects treatment outcome of patients with myelofibrosis. *Haematologica.* 2021;106(9):2384–96.
 45. Ivanovski O, Kulkeaw K, Nakagawa M, Sasaki T, Mizuochi C, Horio Y, Ishitani T, Sugiyama D. Characterization of kidney marrow in zebrafish (*Danio rerio*) by using a new surgical technique. *Prilozi.* 2009;30(2):71–80.
 46. Kusku Cabuk F, Sar M, Canoglu D, Dural C, Gunes ME. Reticulin staining pattern in the differential diagnosis of benign parathyroid lesions. *J Endocrinol Invest.* 2020;43(11):1571–6.
 47. Wang JC, Sindhu H, Chen C, Kundra A, Kafeel MI, Wong C, Lichter S. Immune derangements in patients with myelofibrosis: the role of Treg, Th17, and sIL2Ralpha. *PLoS ONE.* 2015;10(3):e0116723.
 48. Kapor S, Momcilovic S, Kapor S, Mojsilovic S, Radojkovic M, Apostolovic M, Filipovic B, Gotic M, Cokic V, Santibanez JF. Increase in frequency of myeloid-derived suppressor cells in the bone marrow of Myeloproliferative Neoplasms: potential implications in myelofibrosis. *Adv Exp Med Biol.* 2023;1408:273–90.
 49. Wang JC, Kundra A, Andrei M, Baptiste S, Chen C, Wong C, Sindhu H. Myeloid-derived suppressor cells in patients with myeloproliferative neoplasm. *Leuk Res.* 2016;43:39–43.
 50. de Graaf CA, Metcalf D. Thrombopoietin and hematopoietic stem cells. *Cell Cycle.* 2011;10(10):1582–9.
 51. Chen J, Zhu H, Yin Y, Jia S, Luo X. Colorectal cancer: metabolic interactions reshape the tumor microenvironment. *Biochim Biophys Acta Rev Cancer.* 2022;1877(5):188797.
 52. Giallongo C, Dulcamare I, Tibullo D, Del Fabro V, Vicario N, Parrinello N, Romano A, Scandura G, Lazzarino G, Conticello C, Li G, Volti AM, Amorini G, Musumeci M, Di Rosa F, Polito R, Oteri M, Aguenouz R, Parenti F, Di Raimondo GA, Palumbo. CXCL12/CXCR4 axis supports mitochondrial trafficking in tumor myeloma microenvironment. *Oncogenesis.* 2022;11(1):6.
 53. He F, Laranjeira AB, Kong T, Lin S, Ashworth KJ, Liu A, Lasky NM, Fisher DA, Cox MJ, Fulbright MC, Antunes-Heck L, Yu L, Brakhane M, Gao B, Sykes SM, D'Alessandro A, Di Paola J, Oh ST. Multiomic profiling reveals metabolic alterations mediating aberrant platelet activity and inflammation in myeloproliferative neoplasms. *J Clin Invest.* 2024;134(3).
 54. Xia H, Wang W, Crespo J, Kryczek I, Li W, Wei S, Bian Z, Maj T, He M, Liu RJ, He Y, Rattan R, Munkarah A, Guan JL, Zou W. Suppression of FIP200 and autophagy by tumor-derived lactate promotes naive T cell apoptosis and affects tumor immunity. *Sci Immunol.* 2017;2(17).
 55. Husain Z, Huang Y, Seth P, Sukhatme VP. Tumor-derived lactate modifies antitumor immune response: effect on myeloid-derived suppressor cells and NK cells. *J Immunol.* 2013;191(3):1486–95.
 56. Malara A, Gruppi C, Abbonante V, Cattaneo D, De Marco L, Massa M, Iurlo A, Gianelli U, Balduini CL, Tira ME, Muro AF, Chauhan AK, Rosti V, Barosi G, Balduini A. EDA fibronectin-TLR4 axis sustains megakaryocyte expansion and inflammation in bone marrow fibrosis. *J Exp Med.* 2019;216(3):587–604.
 57. Yao S, Chai H, Tao T, Zhang L, Yang X, Li X, Yi Z, Wang Y, An J, Wen G, Jin H, Tuo B. Role of lactate and lactate metabolism in liver diseases (review). *Int J Mol Med.* 2024;54(1).

58. Gu L, Liao P, Liu H. Cancer-associated fibroblasts in acute leukemia. *Front Oncol.* 2022;12:1022979.
59. Myerson M, Christensen JC, Steck JK, Schuberth JM. Avascular necrosis of the foot and ankle. *Foot Ankle Spec.* 2012;5(2):128–36.
60. Agarwal M, Goheen M, Jia S, Ling S, White ES, Kim KK. Type I Collagen Signaling regulates Opposing Fibrotic pathways through alpha(2)beta(1) Integrin. *Am J Respir Cell Mol Biol.* 2020;63(5):613–22.
61. Veidal SS, Karsdal MA, Vassiliadis E, Nawrocki A, Larsen MR, Nguyen QH, Hagglund P, Luo Y, Zheng Q, Vainer B, Leeming DJ. MMP mediated degradation of type VI collagen is highly associated with liver fibrosis—identification and validation of a novel biochemical marker assay. *PLoS ONE.* 2011;6(9):e24753.
62. Wang Y, Jiao L, Qiang C, Chen C, Shen Z, Ding F, Lv L, Zhu T, Lu Y, Cui X. The role of matrix metalloproteinase 9 in fibrosis diseases and its molecular mechanisms. *Biomed Pharmacother.* 2024;171:116116.
63. Ma D, Zhang J, Lin HF, Italiano J, Handin RI. The identification and characterization of zebrafish hematopoietic stem cells. *Blood.* 2011;118(2):289–97.
64. Leon C, Evert K, Dombrowski F, Pertuy F, Eckly A, Laeuffer P, Gachet C, Greinacher A. Romiplostim administration shows reduced megakaryocyte response-capacity and increased myelofibrosis in a mouse model of MYH9-RD. *Blood.* 2012;119(14):3333–41.
65. Bianchi E, Rontautoli S, Tavernari L, Mirabile M, Pedrazzi F, Genovese E, Sartini S, Dall’Ora M, Grisendi G, Fabbiani L, Maccaferri M, Carretta C, Parenti S, Fantini S, Bartalucci N, Calabresi L, Balliu M, Guglielmelli P, Potenza L, Tagliafico E, Losi L, Dominici M, Luppi M, Vannucchi AM, Manfredini R. Inhibition of ERK1/2 signaling prevents bone marrow fibrosis by reducing osteopontin plasma levels in a myelofibrosis mouse model. *Leukemia.* 2023;37(5):1068–79.
66. Kuter DJ, Mufti GJ, Bain BJ, Hasserjian RP, Davis W, Rutstein M. Evaluation of bone marrow reticulin formation in chronic immune thrombocytopenia patients treated with romiplostim. *Blood.* 2009;114(18):3748–56.
67. Contreras-Baeza Y, Sandoval PY, Alarcon R, Galaz A, Cortes-Molina F, Alegria K, Baeza-Lehnert F, Arce-Molina R, Guequen A, Flores CA, San Martin A, Barros LF. Monocarboxylate transporter 4 (MCT4) is a high affinity transporter capable of exporting lactate in high-lactate microenvironments. *J Biol Chem.* 2019;294(52):20135–47.
68. Dell’Anno I, Barone E, Mutti L, Rassl DM, Marciniak SJ, Silvestri R, Landi S, Gemignani F. Tissue expression of lactate transporters (MCT1 and MCT4) and prognosis of malignant pleural mesothelioma (brief report). *J Transl Med.* 2020;18(1):341.

Publisher’s note

Springer Nature remains neutral with regard to jurisdictional claims in published maps and institutional affiliations.